

Provided for non-commercial research and education use.
Not for reproduction, distribution or commercial use.



This article appeared in a journal published by Elsevier. The attached copy is furnished to the author for internal non-commercial research and education use, including for instruction at the authors institution and sharing with colleagues.

Other uses, including reproduction and distribution, or selling or licensing copies, or posting to personal, institutional or third party websites are prohibited.

In most cases authors are permitted to post their version of the article (e.g. in Word or Tex form) to their personal website or institutional repository. Authors requiring further information regarding Elsevier's archiving and manuscript policies are encouraged to visit:

<http://www.elsevier.com/copyright>



Contents lists available at ScienceDirect

Applied Surface Science

journal homepage: www.elsevier.com/locate/apsusc

Characterization of DC reactive magnetron sputtered NiO films using spectroscopic ellipsometry

T.C. Peng^{a,c}, X.H. Xiao^{a,b,c,*}, X.Y. Han^d, X.D. Zhou^{a,c}, W. Wu^{a,c}, F. Ren^{a,c}, C.Z. Jiang^{a,c,*}

^a Key Laboratory of Artificial Micro- and Nano-structures of Ministry of Education, Wuhan University, Wuhan 430072, PR China

^b State Key Laboratory of Electronic Thin Films and Integrated Devices, University of Electronic Science and Technology of China, Chengdu 610054, PR China

^c Center for Electron Microscopy, School of Physics and Technology, Wuhan University, Wuhan 430072, PR China

^d School of Physics, Huazhong University of Science and Technology, Wuhan 430074, PR China

ARTICLE INFO

Article history:

Received 9 December 2010

Received in revised form 30 January 2011

Accepted 30 January 2011

Available online 23 February 2011

Keywords:

NiO films

Spectroscopic ellipsometry

Tauc–Lorentz dispersion function

ABSTRACT

Thin NiO films were deposited at 500 °C on n-type Si(1 1 1) by a DC reactive magnetron sputtering in a gas mixture of oxygen and argon. The ratio between the flow rates of oxygen and argon was respectively set at 1:4, 1:2, and 1:1. The dependence of structures and optical properties of NiO films were investigated using grazing incidence X-ray diffraction and spectroscopic ellipsometry in the spectral region of 1.5–5.0 eV. Ni-rich NiO films were obtained when the ratio between the flow rates of oxygen and argon was 1:4 and 1:2 in sputtering process. And when the ratio was 1:1, a relatively pure NiO film was formed. The partial pressure of oxygen could significantly influence the thickness and roughness of films. Refractive index n , extinction coefficient k , and direct gap energy and indirect gap energy of the NiO films were also subject to the influence of the partial pressure of oxygen.

© 2011 Elsevier B.V. All rights reserved.

1. Introduction

NiO is attractive for its physical properties such as electrochromism [1], gas and moisture sensitivities [2–4], antiferromagnetism, and p-type transparent conduction [5]. In addition, NiO films have also shown good resistance switching characteristics, such as large resistance change induced by external electric fields [6–7]. Recent research on the resistance switching characteristics of NiO thin film in combination with a metal–insulator–metal (MIM) structure has suggested the possibility of their potential application in the next generation nonvolatile resistive random access memory devices [8–10]. Therefore, great attention has been drawn to the growth of nickel oxide films recently. DC reactive magnetron sputtering technique is an easy approach to the growth of high quality NiO films and MIM structure devices. In the DC reactive magnetron sputtering process, the partial pressure of oxygen is a key condition for growing NiO films. The structure and properties of NiO films will be affected by the flow-rate ratio of oxygen. Spectroscopic ellipsometry (SE) is a powerful optical characterization technique for the determination of the optical properties of thin films. In this work, SE was employed to investigate the influence of partial pressure of oxygen on optical properties of thin NiO films grown on opaque Si substrates through DC reactive magnetron sputtering.

2. Materials and methods

The NiO films were deposited from a Ni target (ca.50 mm in diameter, thickness of 3 mm, and 99.99% pure) onto n-type Si(1 1 1) by a DC reactive magnetron sputtering system at (ULVAC, ACS-4000-C4) 500 °C. The value of the substrate–target distance was 150 mm. Sputtering was performed at a constant power of 120 W for 2 h. Gas mixtures of oxygen and argon with a ratio of 1:4, 1:2 and 1:1 were respectively used as the sputtering gas with a total pressure of 0.78 Pa, and the samples were labeled #1–3. Optical properties of thin NiO films were characterized with the SE method. A spectroscopic ellipsometer (SOPRA GES-5E EVOLUTION) was used to acquire spectra in the visible–UV range from 1.55 to 4.96 eV. The ellipsometric angle Ψ and phase difference Δ were recorded at an incidence angle of 75°. The surface morphology of the films was observed by means of atomic force microscopy (AFM) on a SHIMADZU SPM-9500J3. The structure and crystallinity of the films were investigated by grazing incidence X-ray diffraction (GIXRD) with a PANalytical B.V X'Pert PRO, which was operated with monochromatic CuK α radiation source ($\lambda = 0.15418$ nm) in the step scanning mode with steps of 0.02° at a scan speed of 4 s/step.

3. Results and discussion

Fig. 1 shows the GIXRD diffraction patterns which are recorded for sample #1–3 prepared with different flow-rate ratios of oxygen to argon. The rock salt of NiO and the fcc structure of Ni are identified in sample #1 and sample #2. For sample #3, only the rock salt

* Corresponding authors at: Key Laboratory of Artificial Micro- and Nano-structures of Ministry of Education, Wuhan University, Bayi Road, Wuhan 430072, PR China.

E-mail addresses: xxh@whu.edu.cn (X.H. Xiao), czjiang@whu.edu.cn (C.Z. Jiang).

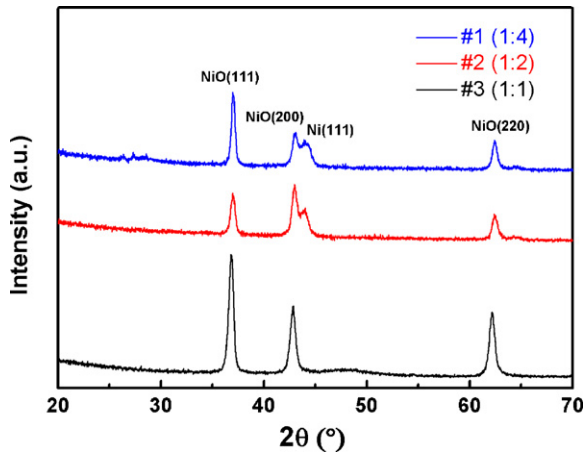


Fig. 1. Grazing incidence X-ray diffraction patterns for sample #1–3.

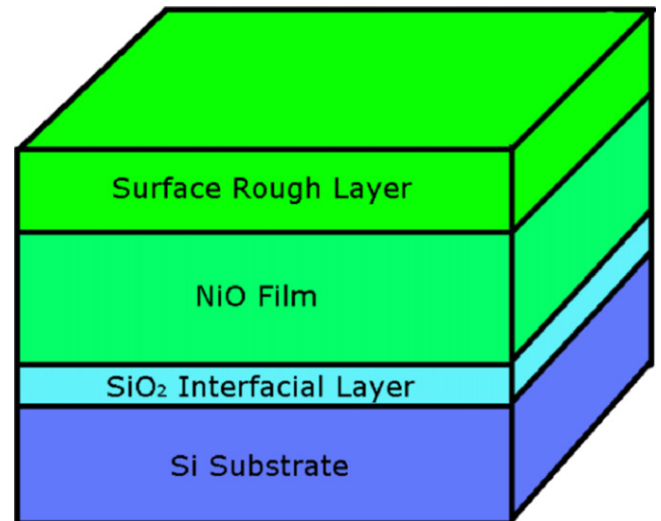


Fig. 2. Structural models for NiO films on Si substrate.

of NiO is identified. All of the samples show the presence of diffraction peaks from the (1 1 1), (2 0 0), and (2 2 0) lattice planes of the NiO lattice. The presence of peaks from the Ni(1 1 1) plane indicates that there are a few Ni metal clusters in sample #1 and sample #2. It can be concluded that no pure NiO film will be formed in the experimental conditions of sample #1 and sample #2. In the DC reactive sputtering process, the Ni clusters are difficult to be fully oxidized due to lack of oxygen. With the increasing partial pressure of oxygen, the Ni metal clusters are fully oxidized to NiO. Hence, the peaks from Ni lattice planes are not found in the diffraction pattern of sample #3.

The Tauc–Lorentz (TL) dispersion function [11–13] is employed to characterize the dielectric function of the NiO films, which is expressed as follows:

$$\epsilon_2(E) = \begin{cases} \frac{AE_0C(E - E_g)^2}{(E^2 - E_g^2)^2 + C^2E^2} \frac{1}{E}, & (E > E_g) \\ 0, & (E < E_g) \end{cases}$$

and

$$\epsilon_1(E) = \epsilon_\infty + \frac{2}{\pi} P \int_{E_g}^{\infty} \frac{\xi \epsilon_2(\xi)}{\xi^2 - E^2} d\xi,$$

where ϵ_1 and ϵ_2 are respectively the real part and imaginary part of the dielectric function, A is the amplitude, E_0 is the peak transition energy, C is the broadening term, and E_g is the band gap. P stands for the Cauchy principal part of the integral, and an additional fitting parameter ϵ_∞ is included. A simple three-layer model is used to represent NiO films on Si substrates, as illustrated in Fig. 2. The surface rough layer is modeled through Bruggeman effective medium approximation [14]. The variables in the fitting procedure include the layer thickness and all TL parameters. The fitting quality is good when a simple TL dispersion function is used.

Fig. 3 shows the experimental (dot symbols) and fitted (line) spectroscopic spectra of $\tan \psi$ (red) and $\cos \Delta$ (blue) as a function of the photon energy of the samples. (For interpretation of the references to color in this text, the reader is referred to the web version of the article.) It can be seen that a good agreement between the experimental and fitted spectra are obtained. This means that the TL dispersion function works well and the physical and optical properties of the NiO films can be exactly determined by the best-fitted results. All of the layer thicknesses and the TL parameter values obtained from data fitting have been summarized in Table 1.

The fitted results are shown in Table 1. t_1 , t_2 and t_3 are the thicknesses of surface rough layer, NiO film, and SiO₂ interfacial layer, respectively. The thickness of NiO films can be obtained by $t_1 + t_2$,

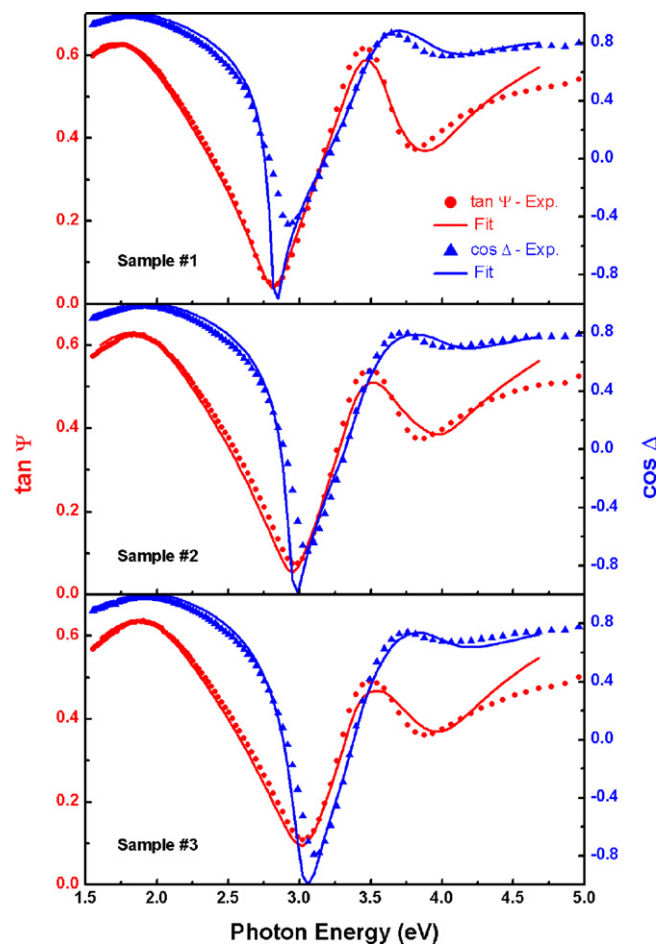


Fig. 3. Experimental and fitted ellipsometric, $\tan \psi$ and $\cos \Delta$, of sample #1–3.

Table 1

Compilation of the fitted results for all the samples using Tauc–Lorentz dispersion function. t_1 , t_2 and t_3 are the thicknesses of surface rough layer, NiO film, and SiO₂ interfacial layer.

Sample	t_1 (nm)	t_2 (nm)	t_3 (nm)	A (eV)	E_0 (eV)	E_g (eV)	C (eV)	ϵ_∞
#1 (1:4)	23.11	59.70	10.72	67.41	4.43	2.51	1.07	2.37
#2 (1:2)	21.70	58.66	7.29	63.07	4.45	2.55	1.03	2.54
#3 (1:1)	15.60	63.11	6.20	59.06	4.37	2.59	1.09	2.89

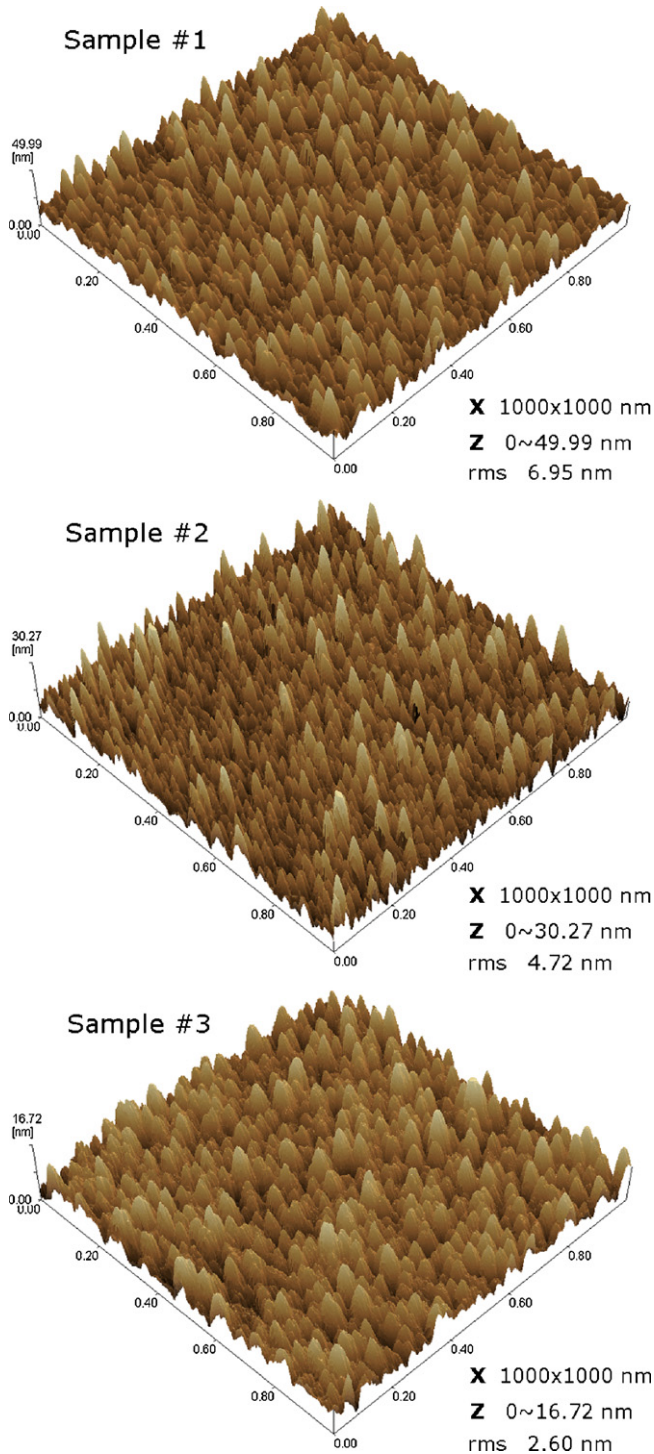


Fig. 4. AFM three-dimensional images of the surface morphology of sample #1–3 over a scan area of $1\ \mu\text{m} \times 1\ \mu\text{m}$.

and the thicknesses of sample #1–3 are respectively 82.81 nm, 80.36 nm, and 78.71 nm, which can lead to the conclusion that the increase in the flow-rate ratio of oxygen to argon results in a decrease of the film thickness. The thicknesses of NiO surface rough layers of sample #1–3 are respectively 23.11 nm, 21.70 nm, and 15.60 nm. Although the thickness of the surface rough layer is not a value for describing the surface roughness, it still reflects the roughness of the NiO film surface to some extent, as a thicker surface rough layer means a rougher surface. According to the fitted results, the increase in partial pressure of oxygen can reduce the

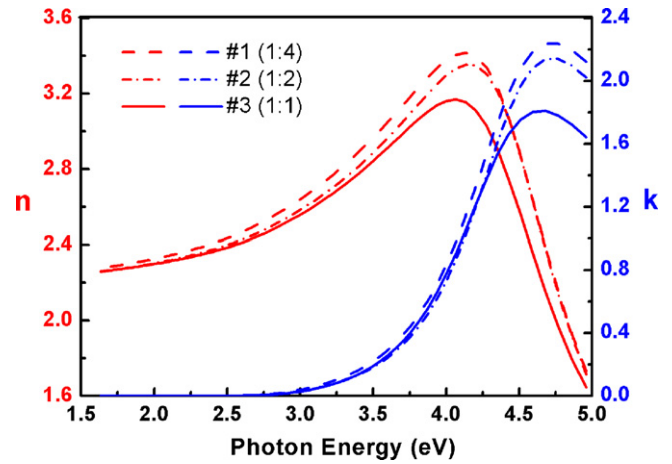


Fig. 5. Spectra of refractive index (n) and extinction coefficient (k) for sample #1–3.

thickness of surface rough layer in the three-layer model. In order to observe the surface morphology and roughness visually, we use AFM to measure the characteristic topography of the samples. As shown in Fig. 4, the root mean square (rms) of roughness of sample #1–3 is 6.96 nm, 4.72 nm, and 2.60 nm respectively. These results show that the surface roughness of these samples will decrease with the increase of partial pressure of oxygen, which are also proved by the fitted results.

The extracted optical constants n and k for sample #1–3 are presented in Fig. 5. The values and energy dependence of refractive index n and extinction coefficient k are similar to those reported for NiO single crystals and films [15–17]. It is found that $n(\#1) > n(\#2) > n(\#3)$ in the visible region and $n(\#1) \approx n(\#2) > n(\#3)$ in the region of 4.3–5 eV. The extinction coefficient k is also larger for sample #1 and sample #2 than for sample #3 in the region of 4.3–5 eV. According to GIXRD analysis, a few Ni clusters are formed in the NiO films of sample #1 and sample #2. The values of the refractive index n and extinction coefficient k of metals are much larger than those of semiconductors. Therefore the mixed Ni clusters may increase the n and k values of the NiO films. Absorption coefficient α of the NiO films can be obtained through the values of extinction coefficient k .

Absorption coefficient α of the NiO films can be obtained by $\alpha = 4\pi k/\lambda$, where λ is the wavelength of the incident light. Fig. 6 shows the spectral variation of absorption coefficient α as a function of the photon energy of these samples. It is observed that α rises abruptly, hitting values of the $10^6\ \text{cm}^{-1}$ order in the UV region.

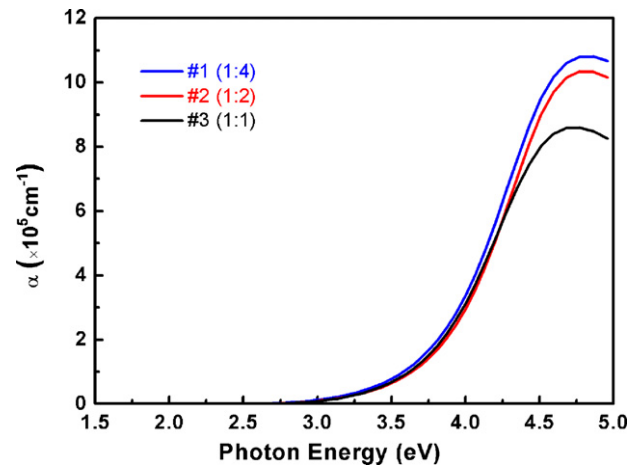


Fig. 6. The absorption coefficient (α) vs. photon energy for sample #1–3.

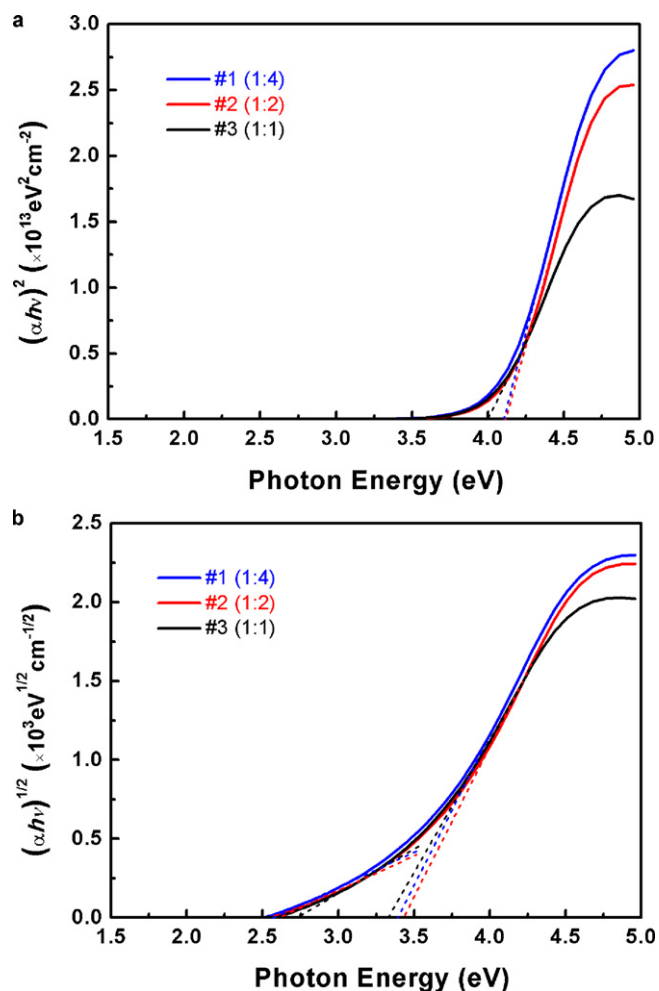


Fig. 7. Plots of $(\alpha h\nu)^2$ (a) and $(\alpha h\nu)^{1/2}$ (b) vs. $h\nu$ for sample #1–3.

This abrupt rise is attributed to band gap absorption of NiO films. Based on the optical absorption spectra, the nature of optical transition can be determined. The optical band gap E_g can be calculated using the well-known relation $\alpha h\nu = A(h\nu - E_g)^m$, where A is a constant, $h\nu$ is the photon energy, and m depends on transition nature. Thus the dependence of $(\alpha h\nu)^{1/m}$ on photon energy should be linear. For the presently studied films, the best fit of $(\alpha h\nu)^{1/m}$ versus $h\nu$ is obtained with $m = 1/2$ and 2. The extrapolation of the linear part of the curve to zero absorption coefficient shows that the investigated samples are characterized by direct and indirect interband transition. Fig. 7(a) shows the variation of $(\alpha h\nu)^2$ versus $h\nu$ for all the samples. The direct interband gap of sample #3 is 4.05 eV, which fully agrees with the approximate value of 4 eV reported for the bulk NiO [18]. The direct interband gaps of sample #1 and sample #2 are nearly equal to 4.10 eV. The direct interband gap of sample #3, which is different from those of sample #1 and sample #2, may also be caused by Ni clusters in the NiO films. The partial pressure of oxygen in the sputtering process will significantly affect width of the energy gap.

Fig. 7(b) shows the variation of $(\alpha h\nu)^{1/2}$ versus $h\nu$ for all the samples. The wave vector K for the lowest energy state in the conduction band is different from that for the highest energy state in the valence band. Consequently, the electrons, which transfer from the valence band to the conduction band, will have different phonon energies E_p due to the change in their wave vectors. In order to maintain the momentum, energy is either supplied by the crystal lattice or given up to it; in other words, one or more phonons

are emitted or absorbed while the photon is absorbed. The optical absorption data is also analyzed as evidence for allowed indirect transitions based on the following [19]:

$$\alpha h\nu = B(h\nu - E_{gind} \pm E_p)^2$$

where B is a constant, E_{gind} is the indirect energy gap (minimum gap between conductor band and valance band), and E_p is the energy of the absorbed (+) or emitted (−) phonons. In Fig. 7(b), each plot may be resolved into two distinct straight line portions. The straight line obtained at lower photon energies corresponds to the phonon absorption process and cuts the energy axis at $(E_{gind} - E_p)$. The other lines which represent the dependence in the relatively higher energy range correspond to a phonon emission process and cut the energy axis at $(E_{gind} + E_p)$. From the energy intercepts, the values of E_{gind} and E_p for all samples have been calculated. The E_{gind} values of sample #1–3 are about 3.00 eV, 3.03 eV, and 3.05 eV respectively. Hence, the partial pressure of oxygen in the sputtering process can also influence the indirect gap energy of these samples.

4. Conclusion

We prepared the NiO films on Si substrate with a DC reactive magnetron sputtering system. The Ni-rich NiO films and relatively pure NiO films can be obtained by controlling the flow-rate ratio of oxygen to argon. The phases and structures of these films were determined by GIXRD. Spectroscopic ellipsometric analyses were employed to investigate the information of the unique optical properties of the NiO films on the opaque substrates. The results show that there are a few incomplete oxidized Ni clusters in the samples grown in oxygen and argon with ratios of 1:4 and 1:2. When the flow-rate ratio of oxygen to argon reaches 1:1, relatively pure NiO films can be obtained. The increase in the partial pressure of oxygen will result in a decrease of the film thickness and reduce the roughness of the films. The mixed Ni clusters may increase the n and k values of the NiO films. The direct gap energy of the sample grown in oxygen and argon with ratios of 1:4, 1:2, and 1:1 are respectively 4.10, 4.10, and 4.05 eV, and the indirect energy gap are respectively 3.00, 3.03, and 3.05 eV. The partial pressure of oxygen in the sputtering process can both influence the direct and indirect gap energy of these samples. NiO films are of particular significance for resistive random access memory device technology. The Ni-rich NiO film and relatively pure NiO film samples have both shown significant and different resistive switching properties in our resent ongoing experiment. The spectroscopic ellipsometric analyses can provide some unique information, whose importance for device technology needs to be further investigated.

Acknowledgements

The author thanks the National Basic Research Program of China (973 Program, no. 2009CB939704), the National Nature Science Foundation of China (nos. 10905043, 11005082), the Specialized Research Fund for the Doctoral Program of Higher Education (no. 20100141120042), Young Chenguang Project of Wuhan City (nos. 200850731371, 201050231055), and the Fundamental Research Funds for the Central Universities.

References

- [1] C.G. Granqvist, Handbook of Inorganic Electrochromic Materials, Elsevier, Amsterdam, 2002, p. 339.
- [2] I. Hotovy, V. Rehacek, P. Siciliano, S. Capone, L. Spiess, Thin Solid Films 418 (2002) 9–15.
- [3] A. Neubecker, T. Pompl, T. Doll, W. Hansch, I. Eisele, Thin Solid Films 310 (1997) 19–23.
- [4] M. Ando, Y. Sato, S. Tamura, T. Kobayashi, Solid State Ionics 121 (1999) 307–311.

- [5] G. Wakefield, P.J. Dobson, Y.Y. Foo, A. Loni, A. Simons, J.L. Hutchison, *Semicond. Sci. Technol.* 12 (1997) 1304–1309.
- [6] S. Seo, M.J. Lee, D.H. Seo, E.J. Jeoung, D.-S. Suh, Y.S. Joung, I.K. Yoo, I.R. Hwang, S.H. Kim, I.S. Byun, J.-S. Kim, J.S. Choi, B.H. Park, *Appl. Phys. Lett.* 85 (2004) 5655–5657.
- [7] Y.-H. You, B.-S. So, J.-H. Hwang, W. Cho, S.S. Lee, T.-M. Chung, C.G. Kim, K.-S. An, *Appl. Phys. Lett.* 89 (2006) 222105–222113.
- [8] I.K. Yoo, B.S. Kang, Y.D. Park, M.J. Lee, Y. Park, *Appl. Phys. Lett.* 92 (2008) 202112–202113.
- [9] J.Y. Son, Y.-H. Shin, *Appl. Phys. Lett.* 92 (2008) 222106–222113.
- [10] C.B. Lee, B.S. Kang, A. Benayad, M.J. Lee, S.-E. Ahn, K.H. Kim, G. Stefanovich, Y. Park, I.K. Yoo, *Appl. Phys. Lett.* 93 (2008) 042115–42123.
- [11] G.E. Jellison Jr., F.A. Modine, *Appl. Phys. Lett.* 69 (1996) 371–373; *Appl. Phys. Lett.* 69 (1996) 2137.
- [12] G. He, L.D. Zhang, G.H. Li, M. Liu, L.Q. Zhu, S.S. Pan, Q. Fang, *Appl. Phys. Lett.* 86 (2005) 232901–232903.
- [13] H.L. Lu, G. Scarel, M. Alia, M. Fanciulli, S.-J. Ding, D.W. Zhang, *Appl. Phys. Lett.* 95 (2009) 012104–12113.
- [14] D.A.G. Bruggemann, *Ann. Phys.* 24 (1935) 636–679.
- [15] R.J. Powell, W.E. Spicer, *Phys. Rev. B* 2 (1970) 2182–2193.
- [16] A.M. Lopez-Beltran, A. Mendoza-Galvan, *Thin Solid Films* 503 (2006) 40–44.
- [17] D. Franta, B. Negulescu, L. Thomas, P.R. Dahoo, M. Guyot, I. Ohlidal, J. Mistrik, T. Yamaguchi, *Appl. Surf. Sci.* 244 (2005) 426–430.
- [18] A.J. Varkey, A.F. Fort, *Thin Solid Films* 235 (1993) 47–50.
- [19] J. Bardeen, F.J. Blatt, L.H. Hall, *Proceedings of Photoconductivity Conference, Atlantic City, Wiley, New York, 1956*, p. 146.